Published in final edited form as:
Int J Parasitol. 2005 July ; 35(8): 851–859. doi:10.1016/j.ijpara.2005.02.017.

In vivo imaging of tissue eosinophilia and eosinopoietic responses to schistosome worms and eggs

Stephen J. Davies[a,1,*], **Steven J. Smith**[b,1], **K.C. Lim**[c], **Hongbing Zhang**[b,2], **Anthony F. Purchio**[b], **James H. McKerrow**[c], and **David B. West**[b]

[a] Department of Microbiology and Immunology, Uniformed Services University of the Health Sciences, 4301 Jones Bridge Road, Room B4104, Bethesda, MD 20814-4799, USA

[b] Xenogen Corporation, 860 Atlantic Ave, Alameda, CA 94501, USA

[c] Tropical Disease Research Unit, Department of Pathology, University of California San Francisco, 513 Parnassus Avenue, San Francisco, CA 94143, USA

Abstract

Using a sensitive transgenic reporter mouse system and in vivo biophotonic imaging techniques, we present a dynamic analysis of eosinophil responses to schistosome infection. Use of this methodology provided previously unattainable detail on the spatial and temporal distribution of tissue eosinophilia and eosinopoietic responses to schistosome worms and eggs. Dramatic hepatic and intestinal eosinophilia in response to the deposition of schistosome eggs, with accompanying eosinopoiesis in the bone marrow, was observed between weeks 8 and 10 p.i., with subsequent downregulation evident by week 11. Contrary to expectations, we also demonstrate that schistosome parasites themselves induce significant intestinal eosinophilia and eosinopoiesis in the bone marrow at very early stages during prepatent infection.

Keywords

Schistosoma; Schistosome; Helminth; Eosinophil; Eosinophilia; Eosinopoiesis; Eosinophil peroxidase

1. Introduction

In view of the biological diversity of parasitic helminths, from platyhelminths to nematodes, these infectious agents are remarkably predictable in their ability to induce $CD4^+$ T helper lymphocytes (T_H cells) to mount type 2 T helper (T_H2) cell responses, characterised by the production of the type 2 cytokines IL-4, IL-5 and IL-13. Consequently, peripheral blood and tissue eosinophilia, driven by IL-5 production, are hallmarks of helminth infection in mammals. A key component of the T_H2 response, IL-5 promotes eosinophilia by stimulating eosinophil differentiation in the bone marrow (eosinopoiesis) and by mediating eosinophil activation (Roboz and Rafii, 1999). In the context of blood fluke infections, the role of IL-5 in eosinophil responses is underlined by the observation that eosinophilia is significantly reduced in schistosome-infected mice treated with neutralising anti-IL-5 antibodies (Sher et al., 1990) and in schistosome-infected IL-5-deficient ($IL\text{-}5^{-/-}$) mice (Brunet et al., 1999). However, despite the prominence of eosinophils during helminth infection, the specific function of these cells in

[*]Corresponding author. Tel.: +1 301 295 3446; fax: +1 301 295 3773. sdavies@usuhs.mil (S.J. Davies).
[1]These authors contributed equally to this work.
[2]Present address: Five Prime Therapeutics, Inc., South San Francisco, CA, USA.

the host response to helminths remains unclear (Behm and Ovington, 2000; Klion and Nutman, 2004).

Various lines of evidence suggest that eosinophils may play a role in the elimination of helminth parasites. For instance, eosinophils have been shown to mediate killing of *Schistosoma mansoni* (David et al., 1980) and other helminths, e.g. *Trichinella spiralis* (Kazura and Grove, 1978) and *Dipetalonema vitae* (Haque et al., 1981), in vitro, by antibody-dependent cellular cytotoxicity (ADCC). Under some circumstances, eosinophils have been found invading sick and dying schistosomes in vivo (Davies et al., 2004). Further, eosinophil granule proteins such as major basic protein (MBP), eosinophil peroxidase (EPX), eosinophil cationic protein (ECP) and eosinophil-derived neurotoxin (EDN) have been shown to be toxic to *Brugia* spp. (Hamann et al., 1990) and to *S. mansoni* (Butterworth et al., 1979) in vitro. Epidemiologic data from human populations in endemic areas suggest that IgE molecules with specificity for schistosome antigens might play a role in mediating immunity to reinfection (Dunne et al., 1992; Hagan et al., 1991; Rihet et al., 1991), possibly by permitting eosinophil-mediated ADCC responses against the parasite. However, direct in vivo evidence from laboratory models demonstrating that eosinophils are involved in eliminating helminths is harder to find. If IgE-mediated ADCC is the primary mechanism by which eosinophils attack helminth parasites in humans, the laboratory mouse may be a poor model for this phenomenon as murine eosinophils, in contrast to human eosinophils, do not express IgE receptors (FcεRI and FcεRII) (de Andres et al., 1997).

Interestingly, recent evidence indicates that eosinophils may play an important role in initiating T_H2 responses to helminths by providing a source of IL-4 during the early stages of the type 2 response. *S. mansoni* eggs and *Nippostrongylus brasiliensis* larvae have both been shown to rapidly recruit IL-4-producing eosinophils to the site of infection (Sabin et al., 1996; Shinkai et al., 2002; Voehringer et al., 2004) and in the case of the latter helminth, this property of eosinophils has also been shown to be independent of T cells (Shinkai et al., 2002; Voehringer et al., 2004).

To gain insights into the role of eosinophils during helminth infection, we sought to develop a comprehensive picture of eosinophil responses to schistosome infection by establishing the spatial and temporal distribution of these cells throughout the course of infection. Because traditional histological detection and enumeration of eosinophils is laborious and insensitive, we made use of transgenic mice that express the luciferase reporter gene driven by the eosinophil-specific *EPX* promoter (Yamaguchi et al., 1994) to identify and quantify eosinophils in vivo in living animals. In these reporter mice (*EPX-luc* mice), the distribution and accumulation of eosinophils in live animals can be monitored by administering luciferase substrate and analyzing the intensity and anatomical distribution of the resulting in vivo bioluminescence. To sensitively monitor the effect of helminth infection on the spatial and temporal distribution of eosinophils in mice and the effect of helminth infection on their distribution, *EPX-luc* mice were infected with *S. mansoni* and the distribution and accumulation of eosinophils was monitored with reference to non-infected *EPX-luc* mice. Our results provide a more dynamic and detailed image of helminth-induced eosinophilia and eosinopoietic responses than was previously possible. We also show that, contrary to expectations, eosinopoiesis and tissue eosinophilia occur well before the onset of parasite oviposition, during the prepatent phase of the infection.

2. Materials and methods

2.1. Animals

The *EPX-luc* transgenic construct (Fig. 1A) was generated using a 9.8 kb fragment of the mouse eosinophil peroxidase (*EPX*) promoter (Gharib et al., 1999;Yamaguchi et al., 1994), subcloned

from a mouse bacterial artificial chromosome (BAC) clone (BAC number P23-193P5; GenBank accession no. AC019272) that was inserted into the pGL3-Basic vector (Promega, Madison, WI). This 9.8 kb mouse genomic DNA fragment was used in an attempt to capture all transcriptional control elements of the *EPX* promoter region and accurately reflect the endogenous *EPX* gene expression. An 800-bp fragment containing the human globin intron II (GenBank accession no. L48931) cloned from human genomic DNA was then inserted between the *EPX* promoter region and the luciferase gene to increase transgene expression and mRNA stability (Brinster et al., 1988;Collis et al., 1990;Ellis et al., 1993). Hemizygous FVB/N-Tg (*EPX-luc*)Xen (abbreviated hereafter as *EPX-luc*) transgenic mice, expressing luciferase under the control of the *EPX* promoter, were generated by DNA microinjection into FVB/N donor embryos and maintained in the FVB/N background. Parallel experiments were performed with two independent lines of *EPX-luc* mice—*EPX334-luc* and *EPX339-luc*. Because similar results were obtained with both lines, only data obtained with the *EPX334-luc* line are shown. All experimental protocols were approved by the Institutional Animal Care and Use Committee of Xenogen Corporation and conformed to principles in the Guide for the Care and Use of Laboratory Animals (Institute of Laboratory Animals Resource, National Research Council, DHHS, 1996). *EPX-luc* hemizygous mice were group-housed in Techniplast microisolator caging and fed standard pelleted rodent chow (Dean's Animal Feeds, Belmont, CA). Water and food were supplied ad libitum. The light/dark cycle was 12 h on and 12 h off, with lights on at 07:00, and room temperature was maintained at 25 °C.

2.2. Infection with *S. mansoni*

Puerto Rican strain *S. mansoni* was maintained in the laboratory using *Biomphalaria glabrata* snails and golden hamsters *Mesocricetus auratus* as intermediate and definitive hosts, respectively (Smithers and Terry, 1965). Cercariae harvested from infected *B. glabrata* were used to infect *EPX-luc* hemizygous mice by subcutaneous injection on the left flank. Fifty cercariae were administered to each animal. Control groups of age- and sex-matched *EPX-luc* hemizygous mice were left uninfected.

2.3. In vivo bioluminescent imaging

Infected and uninfected control animals were weighed and then imaged for transgene expression twice per week over an 84-day period. In vivo imaging was performed using the IVIS® Imaging System 100 Series (Xenogen Corp., Alameda, CA) (Becker et al., 2003; Lee et al., 2003; Sadikot et al., 2003; Zhang et al., 2003, 2004). Prior to image collection, animals were anesthetised with isoflurane and the luciferase substrate luciferin was administered by intraperitoneal injection at a dose rate of 150 mg/kg body weight. During image collection the animals were placed on their backs, with their ventral sides facing the camera for detection of the luciferase signal. To facilitate analysis of the anatomical distribution of in vivo bioluminescence, the ventral aspect of each anesthetised animal was divided into four regions of interest (ROI; Fig. 1B), approximating to the sternum and forelimbs (ROI 1), liver (ROI 2), intestine (ROI 3) and hindlimbs (ROI 4). Photons emitted per second (in photons/second/cm^2/steradian) from each ROI were quantified using LivingImage® software (Xenogen Corp.). Optimal luciferase signal intensity of *EPX-luc* animals was detected between 10 and 20 min following luciferin injection.

2.4. Tissue luciferase assays

Groups of one control and two infected mice were euthanised at various time points p.i. and liver, small intestine, and colon were harvested for luciferase expression. Tissues were frozen in liquid nitrogen immediately following dissection, and later homogenised using a tissue homogenizer (Dremel, Inc., Racine, WI) in PBS containing protease inhibitors (Roche Diagnostics GmbH, Mannheim, Germany). Tissue luciferase assays were performed on whole

tissue homogenates using a reagent kit from Pierce, Inc. (Rockford, IL) and measured with a luminometer (TD 20/20, Turner Designs, Sunnyvale, CA). Luciferase assay results, in relative light units (RLU), were normalised for tissue homogenate protein content, as determined by bicinchoninic acid (BCA) protein assay kit (Pierce, Inc., Rockford, IL).

2.5. Histology

Liver, small intestine and colon were fixed in 4% buffered formaldehyde and embedded in paraffin (IDEXX Veterinary Services, West Sacramento, CA). Sections were stained with H&E, Luna's eosinophil granule stain or Sirius Red.

2.6. Statistical analyses

Statistical significance (P) between infected and non-infected mice was determined by non-parametric Mann–Whitney sign rank test. Spearman's correlation (ρ) was used to quantify and assess the statistical significance of associations between bioluminescence of different regions and between in vivo regional bioluminescence and direct measures of in vitro tissue-specific luciferase activity. All analyses were performed using Statview 5.0 (SAS Institute, Cary, NC).

3. Results

3.1. Schistosome egg accumulation induces in vivo bioluminescence in the livers and intestines of EPX-luc mice

Luciferase bioluminescence data from schistosome-infected *EPX-luc* mice were collected from ROI encompassing the sternum and forelimbs (ROI 1), liver (ROI 2), intestine (ROI 3), and hindlimbs (ROI 4) (Fig. 1B). Representative data showing total bioluminescence from uninfected control and infected animals at selected time points p.i. are shown in Fig. 1C. Little or no luciferase signal was detected in uninfected control animals, while infected animals exhibited readily detectable luciferase activity (Fig. 1C).

Dramatic increases in in vivo bioluminescence were detected in both the hepatic (ROI 2) and intestinal (ROI 3) imaging regions at 8 weeks p.i. (Fig. 2A and C). In contrast, no increase in bioluminescence was observed in uninfected *EPX-luc* animals (Fig. 2A and C). This dramatic induction of bioluminescence followed the onset of parasite oviposition at 5–6 weeks p.i. and correlates with the formation of eosinophil-rich T_H2-dependent granulomas around parasite eggs in the liver and intestine (Pearce and MacDonald, 2002). Peak bioluminescence in both the livers and intestines of infected animals was observed at 10 weeks p.i. (Fig. 2A and C), with levels of luciferase activity approximately 5 (intestine, Fig. 2C) to 20 (liver, Fig. 2A) times that observed in the corresponding regions of uninfected mice. Bioluminescence in the hepatic region (ROI 2) differed significantly between infected and uninfected mice for all time points after day 35 p.i. That of the intestinal region (ROI 3) differed significantly by infection status at all time points between days 56 and 70 inclusive. In infected animals, hepatic bioluminescence correlated significantly ($P<0.05$) with intestinal bioluminescence at day 43 ($\rho=0.53$) and from days 56 to 78 inclusive ($0.86\leq\rho\leq0.90$)

3.2. In vivo bioluminescence correlates with in vitro tissue luciferase activity

After normalising for protein content, the results of in vitro luciferase assays on samples of liver tissue showed significantly higher levels of luciferase activity in infected mice compared to control mice (Fig. 3; $P<0.0001$). Further, while a direct relationship between in vitro tissue luciferase activity (expressed as RLU) and in vivo bioluminescence (in photons/s/cm^2/sr) cannot be precisely and quantifiably correlated (i.e. 10 RLUs=2 photons/s/cm^2/sr), there was a strong and highly significant correlation between fold changes in in vitro hepatic luciferase activity and in vivo bioluminescence of the liver (ROI 2; $\rho=0.84$, $P<0.0001$). Moreover, the

change in hepatic luciferase activity in vitro over time (Fig. 3) corresponded closely to that observed for the change in bioluminescence of the liver region (ROI 2; Fig. 2A), with approximately 100-fold increases in in vitro luciferase activity evident by 8 weeks post-infection. Luciferase activity in samples of small intestinal tissue was also significantly higher in the infected mice than the uninfected mice (P=0.007; data not shown). Correspondingly, in vivo bioluminescence of the intestinal region (ROI 3) correlated significantly with luciferase activity of the small intestine (ρ=0.58, P=0.005).

3.3. In vivo bioluminescence correlates with tissue eosinophilia

To confirm that increased in vivo bioluminescence correlates with increased accumulation of eosinophils, samples of liver and intestine exhibiting increased levels of bioluminescence were examined for eosinophils by histology. Tissue sections stained with H&E, Luna's eosinophil granule stain or Sirius Red were compared to optimise eosinophil detection (data not shown). Murine eosinophils were most clearly visualised with H&E (Fig. 4). By histology, eosinophils were virtually undetectable in sections of liver and intestine from uninfected animals (Fig. 4A and D) that exhibited only background bioluminescence (Fig. 2). However, eosinophils were readily detected in the livers and intestines of animals with patent schistosome infection (Fig. 4B, C, E and F). In these animals, tissue eosinophilia was obvious in both the liver (Fig. 4B and C) and intestine (Fig. 4E and F) at time points when levels of in vivo bioluminescence were also significantly elevated (Fig. 2A and C). Thus, in vivo bioluminescence signals from the liver and intestine were associated with the accumulation of eosinophils in those tissues.

3.4. Egg-induced eosinophilia in the liver and intestine is rapidly downregulated

After peak expression at week 10 p.i., in vivo bioluminescence decreased dramatically in both liver (Fig. 2A) and intestine (Fig. 2C) by 11 weeks p.i. Bioluminescence remained higher than in uninfected animals at both anatomic locations until the end of monitoring at day 84 p.i. (Fig. 2A and C), but was reduced compared with the peak of tissue eosinophilia around week 10.

3.5. Prepatent schistosome infection also induces tissue eosinophilia

While in vivo bioluminescence in the liver and intestine was most pronounced at the time of egg accumulation at these sites, detailed analysis of earlier time points also revealed a small but significant increase in bioluminescence associated with prepatent infection at these anatomic locations (Fig. 2B and D). In the liver (Fig. 2B), significantly higher bioluminescence in infected mice was detectable at days 10 (P=0.04) and 28 (P=0.005) p.i. compared with uninfected controls, with measurements at 21 and 35 days exhibiting marginal differences (P=0.11 for both). Bioluminescence intensity approximately double that of uninfected control animals was detected at 4 weeks p.i. (Fig. 2B). In the intestinal region (Fig. 2D), prepatent in vivo bioluminescence was more pronounced, with significant elevations evident at days 10 (P=0.04), 21 (P=0.009) and 28 (P=0.03) p.i. relative to uninfected mice. Throughout this period, bioluminescence intensity in the intestines of infected animals was approximately twice that observed in control animals.

3.6. Schistosome egg deposition induces a pronounced eosinopoietic response which is subsequently downregulated

Because *EPX* promoter activity and EPX protein synthesis is more pronounced during eosinophil development in the bone marrow than in mature eosinophils (Gruart et al., 1992), in vivo bioluminescence in the long bones and sternum was monitored throughout the course of infection as an indicator of eosinopoiesis. In addition to inducing in vivo bioluminescence in the liver and intestine (Fig. 2), where the physical presence of schistosome eggs attracts eosinophil-rich inflammatory infiltrates (Fig. 4), schistosome egg deposition at these distant sites also induced large increases in bioluminescence in the long bones of the hindlimbs (Fig.

5A) and in the sternum and forelimbs (Fig. 5C), indicative of a dramatic eosinopoietic response beginning around 7 weeks p.i. Hence, schistosome eggs induced an eosinopoietic response (Fig. 5A and C) that preceded egg-mediated liver and intestine eosinophilia (Fig. 2A and C) by a week. Subsequent bioluminescence signals from the long bones and sternum displayed similar kinetics to the tissue eosinophilia the liver and intestine, with peak bioluminescent intensity occurring at 10 weeks p.i. when bioluminescent intensities in infected animals were 20–30 times higher than in uninfected controls (Fig. 5A and C). Further paralleling the kinetics of eosinophil accumulation in the intestine and liver, the eosinopoietic response in the long bones and sternum was rapidly downregulated after 10 weeks of infection (Fig. 5A and C), as demonstrated by the rapid decrease in bioluminescence intensity in these regions by 11 weeks p.i. As in the liver and intestine, bioluminescence remained elevated in the long bones and sternum after downregulation, but was substantially less than at the peak of the eosinopoietic response by the end of monitoring at day 84 p.i. (Fig. 5A and C).

3.7. Prepatent schistosome infection induces early eosinopoiesis

Although peak eosinopoietic responses in the long bones and sternum were associated with schistosome egg deposition, significant increases in bioluminescence at sites of eosinopoiesis were detectable much earlier in infection—by day 10 p.i. in the hindlimbs (Fig. 5B) and in the forelimbs and sternum (Fig. 5D). Increases in bioluminescence prior to the onset of oviposition were not as pronounced as later in infection, but were six to seven times greater than the background intensities observed in uninfected control animals at the same time points (Fig. 5B and D). Prepatent infection was therefore responsible for inducing small but significant levels of eosinopoiesis before the end of the second week of infection.

4. Discussion

As reported by others using more conventional techniques (Lenzi et al., 1987), our data show that schistosome egg deposition in the liver and intestine induces dramatic tissue eosinophilia in these organs (Fig. 2) and induces an accompanying eosinopoietic response in the marrow cavities of the long bones and sternum (Fig. 5). These results are to be expected given that eggs are the dominant T_H2 stimulus during schistosome infection (Grzych et al., 1991) and induce the formation of eosinophil-rich circumoval granulomas in the liver and intestine (Pearce and MacDonald, 2002). Specifically, egg-induced IL-5 production, a prominent component of the anti-egg T_H2 response (Grzych et al., 1991), is responsible for egg-induced eosinophilia (Brunet et al., 1999; Sher et al., 1990) and has been shown to induce expression of EPX in the bone marrow during patent schistosome infection (Bystrom et al., 2004). Together these results confirm the utility of the *EPX-luc* reporter mice for detecting and quantifying eosinophilia and eosinopoiesis in vivo. Interestingly, the detailed temporal resolution of our study clearly shows that schistosome egg-induced eosinopoiesis (Fig. 5A and C) precedes liver and intestine eosinophilia (Fig. 2A and C) by a week. Presumably, eosinophil production in the bone marrow must be upregulated before marked eosinophilia in the periphery can be detected.

Schistosome egg-induced granuloma formation is spontaneously downregulated as infection proceeds, such that the size of new granulomas forming around recently deposited eggs in the chronic phase of infection are smaller than those that form earlier, during the acute phase of infection (Cheever et al., 1998). The precise immunological basis for this downregulation is unclear, but appears to be dependent on B cells and functional Fc receptors (Jankovic et al., 1998). The regulatory cytokine IL-10 appears not to be required for downregulation (Wynn et al., 1998), while roles for other regulatory mechanisms such as transforming growth factor-β (TGF-β) signaling and regulatory T cells have not been adequately addressed (Pearce and MacDonald, 2002). As might be expected, our data show that downregulation of granuloma formation was accompanied by a marked reduction in tissue eosinophilia, evident by 11 weeks

p.i. in liver and intestine (Fig. 2A and C). Interestingly, we also show that downregulation of eosinophilia was accompanied by marked downregulation of eosinopoiesis (Fig. 5A and C). As downregulation of granuloma formation is accompanied by downregulation of the T_H2 response and of IL-5 production specifically (Grzych et al., 1991), our data suggest that initial induction of egg-induced eosinophilia and eosinopoiesis and the subsequent downregulation of these responses might all be directly dependent on egg-induced IL-5 production.

While schistosome egg deposition is the primary stimulus for eosinophilia and eosinopoiesis during schistosome infection (Figs. 2A,C and 5A,C), our results clearly show that, contrary to previous accounts (Lenzi et al., 1987), small but significant eosinophilia and eosinopoiesis are also induced by worms alone, prior to the onset of egg production (Figs. 2B,D and 5B,D). For instance, in the intestine (Fig. 2D) and hindlimb long bones (Fig. 5B), significant eosinophilia and eosinopoiesis were evident by as early as 10 days p.i., respectively. The increased sensitivity of our methods for detecting and quantifying eosinophil responses compared to traditional methods likely account for these discrepancies. Unlike their eggs, schistosomes themselves are believed to induce a predominantly T_H1 response (Grzych et al., 1991), with little or no associated IL-5 production, that persists until egg-induced T_H2 responses arise (Pearce et al., 1991). Prepatent eosinophilia and eosinopoiesis might therefore be mediated by low but significant levels of worm-induced IL-5, or by other factors that could be associated with the worm-induced T_H1 response, such as eotaxin (Pearlman et al., 1997), regulated upon activation, normal T expressed and secreted chemokine (RANTES) (Pearlman et al., 1997) or IL-2 (Anderson and Hayes, 1989). These possibilities are under investigation. Of particular interest is that significant eosinophilia was evident in the intestine during prepatency (Fig. 2D) because during this period, developing schistosomes are thought to reside primarily in the liver (Georgi et al., 1986). Sites of immunological activity during prepatency are of particular interest because of the potential roles prepatent responses may play in modulating schistosome development (Davies et al., 2001) and in mediating vaccine-induced immunity. Prepatent intestinal responses to schistosomes and their impact on parasite development are therefore under further investigation.

In conclusion, using a novel in vivo reporter system we have produced a dynamic and detailed characterisation of eosinophil responses to schistosome infection. Contrary to expectations, our results show that schistosome worms themselves rapidly induce tissue eosinophilia and eosinopoietic responses, albeit of lesser magnitude than those induced by schistosome eggs. Our study highlights several areas worthy of further investigation and establishes the usefulness of *EPX-luc* reporter mice and in vivo bioluminescence imaging for studying the unique aspects of immune responses to helminth parasites. Luciferase trans-gene expression driven by other immunologically relevant promoters, such as the IL-4 promoter (Lee et al., 2003), the IL-6 promoter (Zhang et al., 2004), the IL-12 p40 promoter (Becker et al., 2003), the inducible nitric oxide synthase (iNOS) promoter (Zhang et al., 2003) and nuclear factor κ-B (NF-κB)-dependent promoters (Sadikot et al., 2003), combined with in vivo biophotonic imaging techniques, will likely produce more new data on the in vivo activity of immunologically important genes during immune responses to parasites.

Acknowledgments

We thank Sandra Huling for assistance with histology. J.H.M. is supported by the Sandler Family Foundation and S.J.D. is supported by the National Institutes of Health (F32 AI10424 and K22 AI53054; and P30 DK26743 through the UCSF Liver Center).

References

Anderson TD, Hayes TJ. Toxicity of human recombinant interleukin-2 in rats. Pathologic changes are characterized by marked lymphocytic and eosinophilic proliferation and multisystem involvement. Lab Invest 1989;60:331–346. [PubMed: 2784516]

Becker C, Wirtz S, Blessing M, Pirhonen J, Strand D, Bechthold O, Frick J, Galle PR, Autenrieth I, Neurath MF. Constitutive p40 promoter activation and IL-23 production in the terminal ileum mediated by dendritic cells. J Clin Invest 2003;112:693–706. [PubMed: 12952918]

Behm CA, Ovington KS. The role of eosinophils in parasitic helminth infections: insights from genetically modified mice. Parasitol Today 2000;16:202–209. [PubMed: 10782080]

Brinster RL, Allen JM, Behringer RR, Gelinas RE, Palmiter RD. Introns increase transcriptional efficiency in transgenic mice. Proc Natl Acad Sci USA 1988;85:836–840. [PubMed: 3422466]

Brunet LR, Sabin EA, Cheever AW, Kopf MA, Pearce EJ. Interleukin 5 (IL-5) is not required for expression of a Th2 response or host resistance mechanisms during murine schistosomiasis mansoni but does play a role in development of IL-4-producing non-T, non-B cells. Infect Immun 1999;67:3014–3018. [PubMed: 10338513]

Butterworth AE, Wassom DL, Gleich GJ, Loegering DA, David JR. Damage to schistosomula of *Schistosoma mansoni* induced directly by eosinophil major basic protein. J Immunol 1979;122:221–229. [PubMed: 570202]

Bystrom J, Wynn TA, Domachowske JB, Rosenberg HF. Gene microarray analysis reveals interleukin-5-dependent transcriptional targets in mouse bone marrow. Blood 2004;103:868–877. [PubMed: 14525773]

Cheever AW, Jankovic D, Yap GS, Kullberg MC, Sher A, Wynn TA. Role of cytokines in the formation and down-regulation of hepatic circumoval granulomas and hepatic fibrosis in *Schistosoma mansoni*- infected mice. Mem Inst Oswaldo Cruz 1998;93:25–32. [PubMed: 9921320]

Collis P, Antoniou M, Grosveld F. Definition of the minimal requirements within the human beta-globin gene and the dominant control region for high level expression. EMBO J 1990;9:233–240. [PubMed: 2295312]

David JR, Butterworth AE, Vadas MA. Mechanism of the interaction mediating killing of *Schistosoma mansoni* by human eosinophils. Am J Trop Med Hyg 1980;29:842–848. [PubMed: 7435788]

Davies SJ, Grogan JL, Blank RB, Lim KC, Locksley RM, McKerrow JH. Modulation of blood fluke development in the liver by hepatic CD4+ lymphocytes. Science 2001;294:1358–1361. [PubMed: 11701932]

Davies SJ, Lim KC, Blank RB, Kim JH, Lucas KD, Hernandez DC, Sedgwick JD, McKerrow JH. Involvement of TNF in limiting liver pathology and promoting parasite survival during schistosome infection. Int J Parasitol 2004;34:27–36. [PubMed: 14711587]

de Andres B, Rakasz E, Hagen M, McCormik ML, Mueller AL, Elliot D, Metwali A, Sandor M, Britigan BE, Weinstock JV, Lynch RG. Lack of Fc-epsilon receptors on murine eosinophils: implications for the functional significance of elevated IgE and eosinophils in parasitic infections. Blood 1997;89:3826–3836. [PubMed: 9160690]

Dunne DW, Butterworth AE, Fulford AJ, Kariuki HC, Langley JG, Ouma JH, Capron A, Pierce RJ, Sturrock RF. Immunity after treatment of human schistosomiasis: association between IgE antibodies to adult worm antigens and resistance to reinfection. Eur J Immunol 1992;22:1483–1494. [PubMed: 1601036]

Ellis J, Talbot D, Dillon N, Grosveld F. Synthetic human beta-globin 5′HS2 constructs function as locus control regions only in multicopy transgene concatamers. EMBO J 1993;12:127–134. [PubMed: 8428573]

Georgi JR, Wade SE, Dean DA. Attrition and temporal distribution of *Schistosoma mansoni* and *S. haematobium* schistosomula in laboratory mice. Parasitology 1986;93:55–70. [PubMed: 3092171]

Gharib B, Abdallahi OM, Dessein H, De Reggi M. Development of eosinophil peroxidase activity and concomitant alteration of the antioxidant defenses in the liver of mice infected with *Schistosoma mansoni*. J Hepatol 1999;30:594–602. [PubMed: 10207800]

Gruart V, Truong MJ, Plumas J, Zandecki M, Kusnierz JP, Prin L, Vinatier D, Capron A, Capron M. Decreased expression of eosinophil peroxidase and major basic protein messenger RNAs during eosinophil maturation. Blood 1992;79:2592–2597. [PubMed: 1375105]

Grzych JM, Pearce E, Cheever A, Caulada ZA, Caspar P, Heiny S, Lewis F, Sher A. Egg deposition is the major stimulus for the production of Th2 cytokines in murine schistosomiasis mansoni. J Immunol 1991;146:1322–1327. [PubMed: 1825109]

Hagan P, Blumenthal UJ, Dunn D, Simpson AJ, Wilkins HA. Human IgE. IgG4 and resistance to reinfection with *Schistosoma haematobium*. Nature 1991;349:243–245. [PubMed: 1898985]

Hamann KJ, Gleich GJ, Checkel JL, Loegering DA, McCall JW, Barker RL. In vitro killing of microfilariae of *Brugia pahangi* and *Brugia malayi* by eosinophil granule proteins. J Immunol 1990;144:3166–3173. [PubMed: 2324497]

Haque A, Ouaissi A, Joseph M, Capron M, Capron A. IgE antibody in eosinophil- and macrophage-mediated in vitro killing of *Dipetalonema viteae* microfilariae. J Immunol 1981;127:716–725. [PubMed: 7195919]

Jankovic D, Cheever AW, Kullberg MC, Wynn TA, Yap G, Caspar P, Lewis FA, Clynes R, Ravetch JV, Sher A. CD4+ T cell-mediated granulomatous pathology in schistosomiasis is downregulated by a B cell-dependent mechanism requiring Fc receptor signaling. J Exp Med 1998;187:619–629. [PubMed: 9463412]

Kazura JW, Grove DI. Stage-specific antibody-dependent eosinophil-mediated destruction of *Trichinella spiralis*. Nature 1978;274:588–589. [PubMed: 672989]

Klion AD, Nutman TB. The role of eosinophils in host defense against helminth parasites. J Allergy Clin Immunol 2004;113:30–37. [PubMed: 14713904]

Lee GR, Fields PE, Griffin TJ, Flavell RA. Regulation of the Th2 cytokine locus by a locus control region. Immunity 2003;19:145–153. [PubMed: 12871646]

Lenzi HL, Sobral AC, Lenzi JA. “In vivo” kinetics of eosinophils and mast cells in experimental murine schistosomiasis. Mem Inst Oswaldo Cruz 1987;82(Suppl 4):67–76. [PubMed: 3151116]

Pearce EJ, MacDonald AS. The immunobiology of schistosomiasis. Nat Rev Immunol 2002;2:499–511. [PubMed: 12094224]

Pearce EJ, Caspar P, Grzych JM, Lewis FA, Sher A. Downregulation of Th1 cytokine production accompanies induction of Th2 responses by a parasitic helminth *Schistosoma mansoni*. J Exp Med 1991;173:159–166. [PubMed: 1824635]

Pearlman E, Lass JH, Bardenstein DS, Diaconu E, Hazlett FE Jr, Albright J, Higgins AW, Kazura JW. IL-12 exacerbates helminth-mediated corneal pathology by augmenting inflammatory cell recruitment and chemokine expression. J Immunol 1997;158:827–833. [PubMed: 8993000]

Rihet P, Demeure CE, Bourgois A, Prata A, Dessein AJ. Evidence for an association between human resistance to *Schistosoma mansoni* and high anti-larval IgE levels. Eur J Immunol 1991;21:2679–2686. [PubMed: 1936116]

Roboz GJ, Rafii S. Interleukin-5 and the regulation of eosinophil production. Curr Opin Hematol 1999;6:164–168. [PubMed: 10226737]

Sabin EA, Kopf MA, Pearce EJ. *Schistosoma mansoni* egg-induced early IL-4 production is dependent upon IL-5 and eosinophils. J Exp Med 1996;184:1871–1878. [PubMed: 8920874]

Sadikot RT, Han W, Everhart MB, Zoia O, Peebles RS, Jansen ED, Yull FE, Christman JW, Blackwell TS. Selective I kappa B kinase expression in airway epithelium generates neutrophilic lung inflammation. J Immunol 2003;170:1091–1098. [PubMed: 12517978]

Sher A, Coffman RL, Hieny S, Scott P, Cheever AW. Interleukin 5 is required for the blood and tissue eosinophilia but not granuloma formation induced by infection with *Schistosoma mansoni*. Proc Natl Acad Sci USA 1990;87:61–65. [PubMed: 2104985]

Shinkai K, Mohrs M, Locksley RM. Helper T cells regulate type-2 innate immunity in vivo. Nature 2002;420:825–829. [PubMed: 12490951]

Smithers SR, Terry RJ. The infection of laboratory hosts with cercariae of *Schistosoma mansoni* and the recovery of the adult worms. Parasitology 1965;55:695–700. [PubMed: 4957633]

Voehringer D, Shinkai K, Locksley RM. Type 2 immunity reflects orchestrated recruitment of cells committed to IL-4 production. Immunity 2004;20:267–277. [PubMed: 15030771]

Wynn TA, Cheever AW, Williams ME, Hieny S, Caspar P, Kuhn R, Muller W, Sher A. IL-10 regulates liver pathology in acute murine Schistosomiasis mansoni but is not required for immune down-modulation of chronic disease. J Immunol 1998;160:4473–4480. [PubMed: 9574553]

Yamaguchi Y, Zhang D, Sun Z, Albee E, Nagata S, Tenen D, Ackerman S. Functional characterization of the promoter for the gene encoding human eosinophil peroxidase. J Biol Chem 1994;269:19410–19419. [PubMed: 8034708]

Zhang N, Weber A, Li B, Lyons R, Contag PR, Purchio AF, West DB. An inducible nitric oxide synthase-luciferase reporter system for in vivo testing of anti-inflammatory compounds in transgenic mice. J Immunol 2003;170:6307–6319. [PubMed: 12794164]

Zhang J, Dai J, Lu Y, Yao Z, O'Brien CA, Murtha JM, Qi W, Hall DE, Manolagas SC, Ershler WB, Keller ET. In vivo visualization of aging-associated gene transcription: evidence for free radical theory of aging. Exp Gerontol 2004;39:239–247. [PubMed: 15036418]

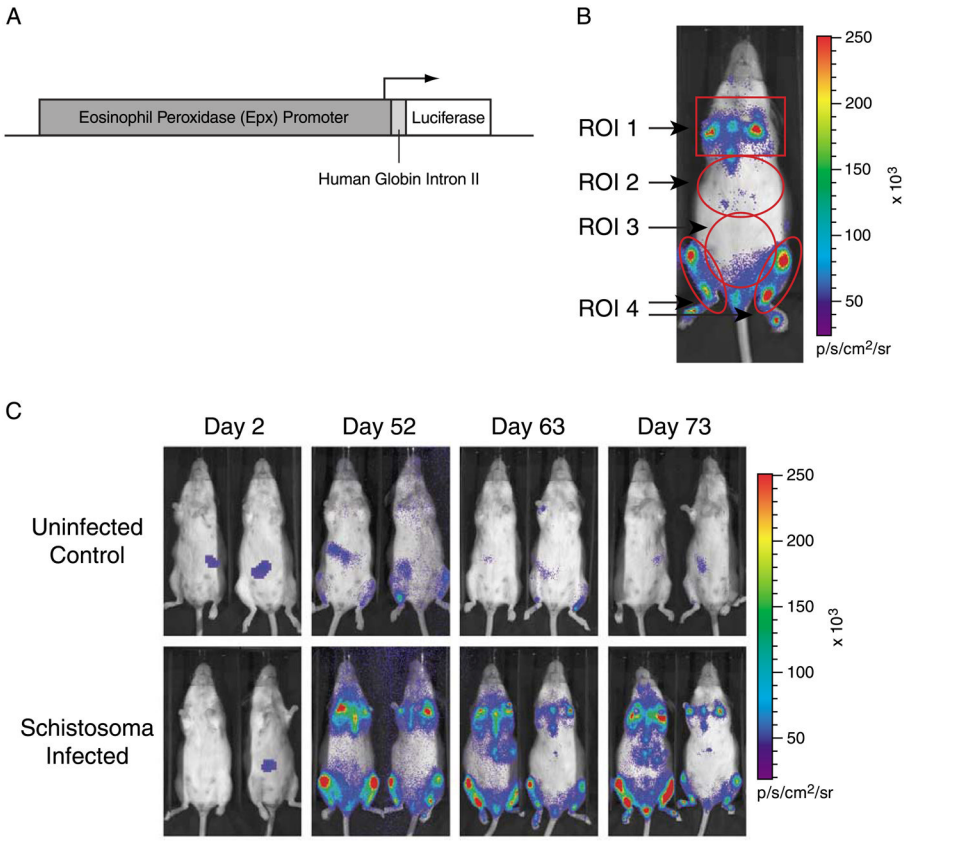

Fig. 1.

In vivo bioluminescence imaging of luciferase reporter gene signal in *EPX-luc* mice. Luciferin was administered to anesthetised *EPX-luc* mice and bioluminescence was detected and quantified 10–20 min later using an IVIS® Imaging System 100 Series. (A) schematic of the transgene construct used to generate *EPX-luc* reporter mice. (B) representative *EPX-luc* animal, at 70 days p.i. with *Schistosoma mansoni*, showing the locations of ROI 1 (sternum and forelimb long bones), ROI 2 (liver), ROI 3 (intestine) and ROI 4 (hindlimb long bones). (C) representative uninfected and schistosome-infected *EPX-luc* animals at various time points p.i. False color overlay represents bioluminescence intensity in photons/s.

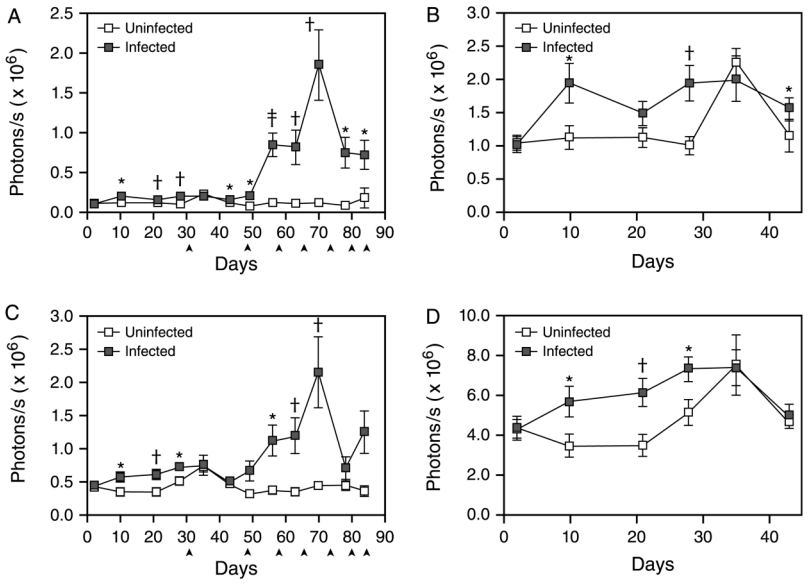

Fig. 2.

In vivo bioluminescence in the livers and intestines of *Schistosoma mansoni*-infected *EPX-luc* mice. In vivo bioluminescence in uninfected and schistosome-infected *EPX-luc* mice was detected twice weekly over the first 12 weeks of infection as described in Fig. 1. Data from all time points were quantified using LivingImage® software and represented graphically. (A) Quantified image data from ROI encompassing the liver (ROI 2) during the 12-week course of the study. (B) Expanded view of liver (ROI 2) data during the first 43 days of the study. (C) Quantified image data from ROI encompassing the intestine (ROI 3) during the 12-week course of the study. (D) Expanded view of intestine (ROI 3) data during the first 43 days of the study. ▲: one control and two infected mice euthanised for histology and in vitro tissue luciferase assays. Time points where statistically significant differences in bioluminescence between infected and uninfected animals were detected by Mann–Whitney sign rank test are denoted by *$P \leq 0.05$; †$P \leq 0.01$; and ‡$P \leq 0.001$. Mean readings±SEM are shown.

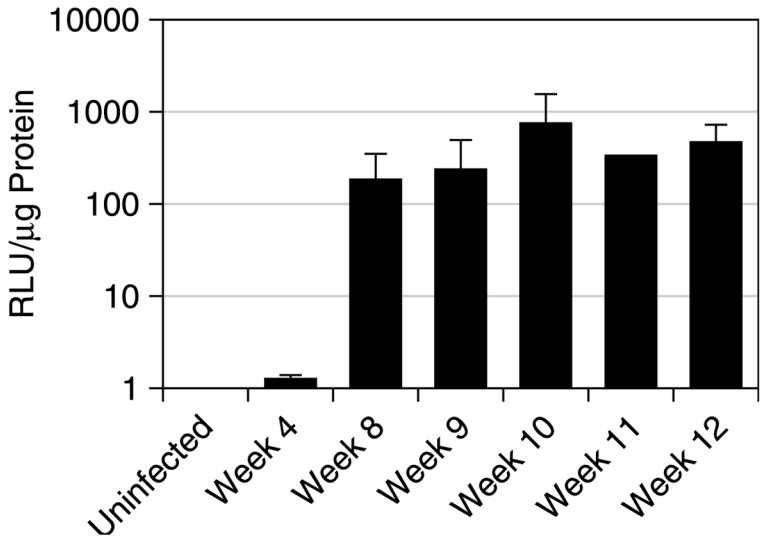

Fig. 3.

In vitro tissue luciferase activity in the livers of uninfected and schistosome-infected *EPX-luc* mice. Samples of liver tissue removed from infected and uninfected *EPX-luc* animals were homogenised and analysed for luciferase activity. Results were normalised against the protein content of the tissue homogenates and expressed in relative light units (RLU)/µg total protein. Mean readings±SEM are shown. Data are representative of at least two independent replicates.

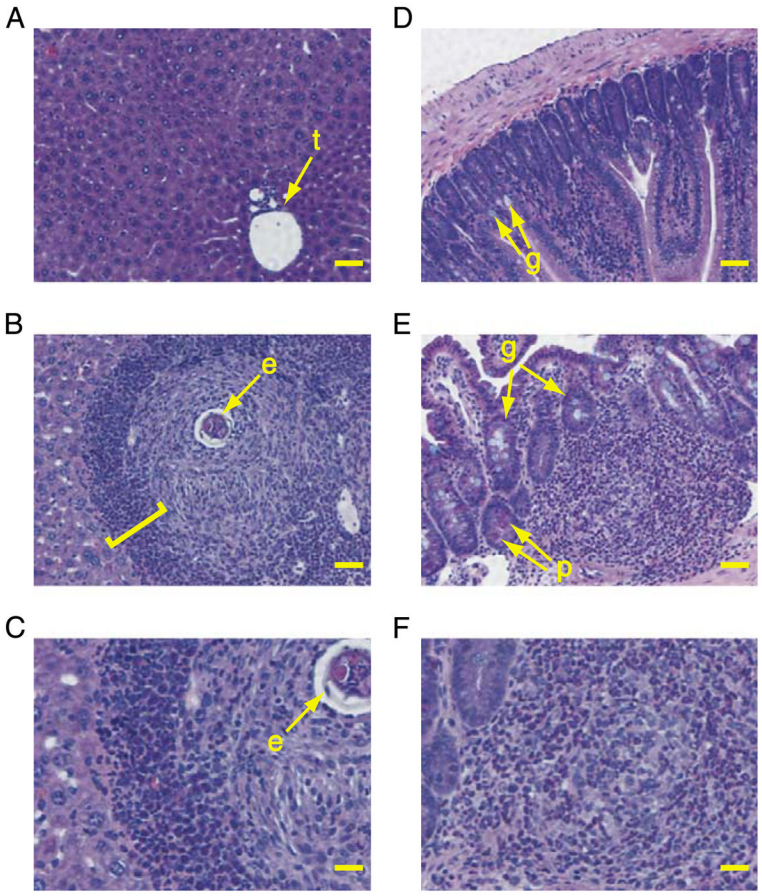

Fig. 4.

Histological detection of eosinophils in tissue sections from uninfected and infected *EPX-luc* mice. Tissue samples from infected and uninfected *EPX-luc* mice were fixed in 4% buffered formaldehyde and embedded in paraffin. Sections were stained with H&E. (A) Liver of uninfected *EPX-luc* mouse. t, portal tract. Scale bar=50 μm. (B) Liver of infected *EPX-luc* mouse at 9 weeks p.i. e, schistosome egg at the center of a granuloma. Square bracket encompasses eosinophil-rich collar around the periphery of the granuloma. Scale bar=50 μm. (C) enlarged portion of section in B, showing many eosinophils within and around the periphery of a circumoval granuloma. Scale bar=25 μm. (D) Small intestine of uninfected *EPX-luc* mouse. g, goblet cells. Scale bar=50 μm. (E) small intestine of infected *EPX-luc* mouse at 9 weeks p.i. Note: dense eosinophil-rich inflammatory infiltrate within the submucosa. g, goblet cells. p, Paneth cells containing large eosinophilic granules. Scale bar=50 μm. (F) Enlarged portion of section in E, showing inflammatory infiltrate containing many eosinophils. Scale bar=25 μm.

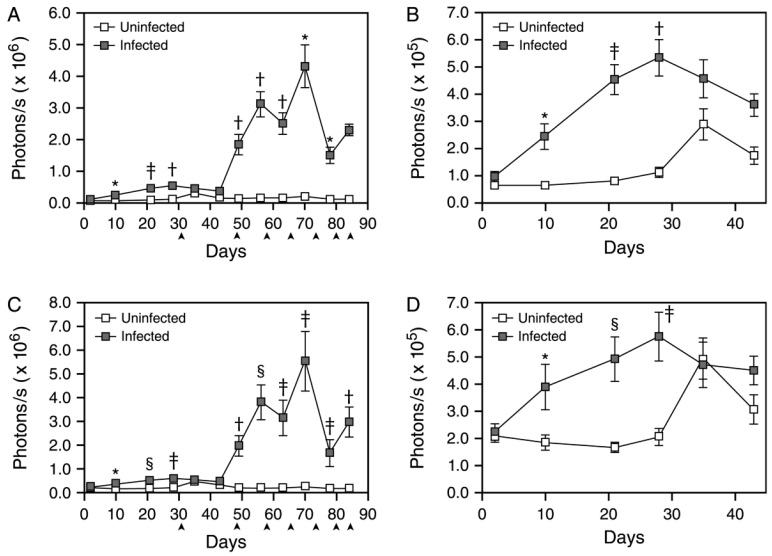

Fig. 5.

In vivo bioluminescence in the long bones and sterna of *Schistosoma mansoni*-infected *EPX-luc* mice. In vivo bioluminescence in uninfected and schistosome-infected *EPX-luc* mice was detected twice weekly over the first 12 weeks of infection as described in Fig. 1. Data from all time points were quantified using LivingImage software and represented graphically. (A) Quantified image data from ROI encompassing the hindlimb long bones (ROI 4) during the 12-week course of the study. (B) Expanded view of hindlimb (ROI 4) data during the first 43 days of the study. (C) Quantified image data from ROI encompassing the forelimbs and sternum (ROI 1) during the 12-week course of the study. (D) Expanded view of forelimb and sternum (ROI 1) data during the first 43 days of the study. ▲: one control and two infected mice euthanised for histology and in vitro tissue luciferase assays. Time points where statistically significant differences in bioluminescence between infected and uninfected animals were detected by Mann–Whitney sign rank test are denoted by *$P \leq 0.05$; †$P \leq 0.01$; ‡ $P \leq 0.001$; and §$P \leq 0.0001$. Mean readings±SEM are shown.